–Regular Paper–

MANIPULABILITY ANALYSIS OF A SNAKE ROBOT WITHOUT A LATERAL CONSTRAINT FOR HEAD POSITION CONTROL

R. Ariizumi and M. Tanaka

ABSTRACT

Two dynamic manipulability criteria of a snake robot with sideways slipping are proposed with the application to head trajectory tracking control in mind. The singular posture, which is crucial in head tracking control, is characterized by the manipulability and examined for families of typical robot shapes. Differences in the singular postures from those of the robot with lateral constraints, which have not been clear in previous studies, are clarified in the analysis. In addition to the examination of local properties using the concept of manipulability, we discuss the effect of isotropic friction as a global property. It is well known that, at least empirically, a snake robot needs anisotropy in friction to move by serpentine locomotion if there are no objects for it to push around. From the point of view of integrability, we show one of the necessary conditions for uncontrollability is satisfied if the friction is isotropic.

Key Words: Controllability, Dynamical model, Head trajectory tracking, Hyper redundant manipulator, Manipulability, Snake robot

I. Introduction

Since the pioneering work of Hirose [1], researchers have been interested in snake robots not only because they have many potential applications [2, 3, 4] but also because they pose great theoretical challenges. From the perspective of control, it is challenging to establish controllability and observability properties because the system is highly nonlinear. Early studies often assumed a lateral constraint; i.e., a constraint that any link, typically equipped with passive wheels, does not slip

Manuscript received July 8, 2008.

R. Ariizumi is with the Department of Mechanical System Engineering, Graduate School of Engineering, Nagoya University, Nagoya 464-8603, Japan, and is the corresponding author (e-mail: ryo.ariizumi@mae.nagoya-u.ac.jp, Phone/Fax: +81-52-789-2746).

M. Tanaka is with the Department of Mechanical and Intelligent Systems Engineering, Graduate School of Information Science and Engineering, The University of Electro-Communications, Tokyo 182-8585, Japan (e-mail: mtanaka@uec.ac.jp).

This work was supported by the ImPACT Program of the Council for Science, Technology and Innovation (Cabinet Office, Government of Japan).

sideways [5, 6]. Under such a velocity constraint, the movement of the robot can be determined by a set of linear equations on velocities. This greatly simplifies the analysis of the robot and has resulted in major findings.

Matsuno and his team [7, 8] closely investigated the conditions required to track the head trajectory. They proved that the simultaneous control of the head velocity and angular velocity of the first link requires the first link not to be subject to the lateral constraint. Links that are not subject to the lateral constraint are associated with joints whose angles are not to be determined directly by commands, which they named shape-controllable points. Using the kinematic redundancy of the shape-controllable points, they proposed a controller based on kinematics and dynamics. Tanaka and Tanaka [9] analyzed singular postures in the case that there are links without lateral constraint. They derived the necessary and sufficient conditions for a wider class of serial-link wheeled manipulators including snake robots. Date et al. [10] extended the concept of dynamic manipulability for manipulators to snake robots with a lateral constraint. They analyzed the head trajectory tracking motion

in terms of manipulability. Studies that assume the lateral constraint are still conducted for more complex tasks [11, 12], to propose novel modeling [13], and to develop a deeper mathematical understanding of a robot [14].

In the case of real snake robots, however, sideways slipping is rather common and many researchers have proposed the modeling, analysis, and control of snake robots with sideways slipping. Most researchers use the serpenoid curve that Hirose [1] proposed as the mathematical model of the shape of snakes. Saito et al. [15] employed viscous and Coulomb friction models and analyzed locomotion using a serpenoid curve from the standpoint of power efficiency. They also proposed a speed control that uses an extension of the serpenoid curve. Ariizumi and Matsuno [16] used a viscous friction model and serpenoid curve to assess the performance of three popular gaits from the point of view of Pareto optimization. Additionally, a viscous friction model has been used to consider the straight path tracking control of the center of mass (CM) of a snake robot [17, 18]. Hicks and Ito [19] proposed an algorithm that generates an optimal gait for a point-to-point control task and showed that their algorithm provides a shape similar to the serpenoid curve.

However, analysis of the controllability of snake robots with sideways slipping is still to be discussed. Because of the nonlinearity of the system, any necessary and sufficient conditions for controllability would be out of reach. Moreover, as is well known, only local properties can be discussed in general. Lilijebäck et al. [20] studied the controllability properties of snake robots, using a dynamic model assuming viscous friction. From the direct observation of the equation of motion, they proved that anisotropy in viscous friction is necessary for the CM of a snake robot to be controllable. They then checked one of the sufficient conditions for accessibility, which is a part of the Lie bracket rank condition. Their analysis revealed that the shape of an arc, in which all joints share the same angle, does not satisfy the necessary condition. As it is well known that arc shapes are singular postures for snake robots with lateral constraints [7, 9, 21, 22], this seems consistent with a limiting case of an infinite coefficient of friction in the lateral direction. However, it is not obvious that these shapes are also singular postures for snake robots with sideways slipping.

In this paper, we propose dynamic manipulability criteria for snake robots with the aim of constructing a head trajectory control. Unlike the control of the CM, the serpenoid curve is not applicable directly to the shape of the robot for head control and it is therefore crucial to understand the singular postures. The formal definition of a singular posture is given in Section III, but here we loosely define it to be the posture from which we cannot accelerate the control point in an arbitrary direction. In terms of understanding the singular posture in snake robots with sideways slipping, the accessibility rank condition used in [20] is too complex and only a sufficient condition for accessibility can be discussed. Therefore, manipulability, which can be calculated easily, is used for this purpose. Although the dynamic manipulability of a snake robot has been proposed in the case that a lateral constraint is imposed [10], the same criterion cannot be applied directly because velocity constraints were used to define the dynamic manipulability. The manipulability is defined by the so-called manipulability ellipsoid that expresses the region of acceleration of the head that is achievable with torque inputs whose norms are less than or equal to unity. However, as we are mainly interested in singular postures, some simplification is possible. As the manipulability expresses only a local structure that is determined only by inertial properties, it is not possible to discuss the effect of friction. The robot cannot be controlled even though the manipulability is not zero if the friction is isotropic, which we clarify by discussing integrability. Although we can only prove the necessary condition for uncontrollability, this will support our intuition based on our observation of snakes. Moreover, we are interested in constructing a head trajectory tracking control that is robust against actuator failure (e.g., when an actuator is unable to provide a torque) in future work. As the first step to this end, we also consider the case of a free joint.

In summary, the contributions of the present study are that we (i) define two dynamic manipulability criteria for the snake robot without a lateral constraint for head trajectory control, (ii) analyze singular postures using the manipulability, and (iii) explain the impossibility of the head trajectory tracking control in the case of isotropic friction. The first two points are also discussed for the case that a joint is free, which is assumed to be a typical case of a malfunctioning actuator.

In what follows, the model of the robot is explained in Section II. Section III defines the dynamic manipulability criteria and Section IV analyzes the criteria. Section V shows that with isotropic friction, the system satisfies a necessary condition to be uncontrollable. In Section VI, a simple simulation is performed to show the usefulness of the manipulability in assessing the singularity and to verify the discussion in Section V. Section VII concludes the paper.

II. Model of a Planar Snake Robot

The equation of motion of a planar snake robot is derived using the Euler–Lagrange method. Details of the partial derivative calculations are available in the literature [16].

2.1. Notation

In this research, we consider an n-link planar snake robot. The schematics of the snake robot are shown in Fig. 1. It is assumed that links are identical; i.e., they have the same mass and length. The CM of a link is assumed to coincide with the geometrical center of the link. Some notations used in the present paper are defined as follows.

l	: Half the length of each link
θ_i	: Orientation of link i
ϕ_i	: Yaw angle of joint i. $\phi_i = \theta_{i+1} - \theta_i$
(x_h, y_h)	: Position of the head
$\boldsymbol{w}$	: $\boldsymbol{w} = [x_h \ \ y_h \ \ \theta_1]^T$
$\boldsymbol{x}_i$	: Position vector of the center of link i, expressed as $\boldsymbol{x}_i = [x_i \ \ y_i]^T$
$\boldsymbol{x}, \boldsymbol{y}$	: $\boldsymbol{x} = [x_1 \ \cdots \ x_n]^T$, $\boldsymbol{y} = [y_1 \ \cdots \ y_n]^T$
$\boldsymbol{\theta}, \boldsymbol{\phi}$	: $\boldsymbol{\theta} = [\theta_1 \ \cdots \ \theta_n]^T$, $\boldsymbol{\phi} = [\phi_1 \ \cdots \ \phi_{n-1}]^T$
$\bar{\boldsymbol{q}}$	: General coordinate, $\bar{\boldsymbol{q}} = [x_h \ \ y_h \ \ \boldsymbol{\theta}^T]^T$

The local coordinates of link i, $O_i - x_i y_i$, are fixed on the CM of link i with inclination of θ_i from the global frame.

Some abuse of the notation of trigonometric functions with vector-valued inputs is defined as

$$\begin{aligned} \cos\boldsymbol{\theta} &= \begin{bmatrix} \cos\theta_1 & \cos\theta_2 & \cdots & \cos\theta_n \end{bmatrix}^T, \\ \sin\boldsymbol{\theta} &= \begin{bmatrix} \sin\theta_1 & \sin\theta_2 & \cdots & \sin\theta_n \end{bmatrix}^T. \end{aligned} \quad (1)$$

Diagonal matrices with trigonometric functions in diagonal entries are often used in what follows:

$$\begin{aligned} C_\theta &= \operatorname{diag}(\cos\theta_1, \ \cos\theta_2, \ \cdots, \ \cos\theta_n), \\ S_\theta &= \operatorname{diag}(\sin\theta_1, \ \sin\theta_2, \ \cdots, \ \sin\theta_n). \end{aligned} \quad (2)$$

2.2. Dynamic Model of a Planar Snake Robot [16]

The positions of CMs of links in the global frame are calculated as

$$\begin{cases} \boldsymbol{x} &= \boldsymbol{1} x_h + K\cos\boldsymbol{\theta} \\ \boldsymbol{y} &= \boldsymbol{1} y_h + K\sin\boldsymbol{\theta} \end{cases}, \quad (3)$$
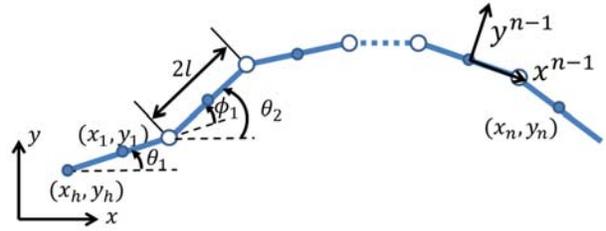

Fig. 1. Schematic of a snake robot with n links and $n-1$ joints

where K and the vector $\boldsymbol{1}$ are defined as

$$K = l \begin{bmatrix} 1 & 0 & \cdots & & 0 \\ 2 & 1 & \cdots & & 0 \\ \vdots & \vdots & \ddots & & \vdots \\ 2 & 2 & \cdots & 2 & 1 \end{bmatrix} \in \mathbb{R}^{n \times n}, \quad (4)$$

$$\boldsymbol{1} = [1 \ 1 \ \cdots \ 1]^T \in \mathbb{R}^n. \quad (5)$$

Because K is a constant matrix, we have

$$\dot{\boldsymbol{x}} = J_{\bar{q}x}\dot{\bar{\boldsymbol{q}}}, \ \ \dot{\boldsymbol{y}} = J_{\bar{q}y}\dot{\bar{\boldsymbol{q}}}, \ \ \dot{\boldsymbol{\theta}} = \begin{bmatrix} O_{n\times2} & I_n \end{bmatrix}\dot{\bar{\boldsymbol{q}}}, \quad (6)$$

where I_k is a $k \times k$ identity matrix and

$$J_{\bar{q}x} = \begin{bmatrix} \boldsymbol{1} & \boldsymbol{0} & -KS_\theta \end{bmatrix}, \ \ J_{\bar{q}y} = \begin{bmatrix} \boldsymbol{0} & \boldsymbol{1} & KC_\theta \end{bmatrix}. \quad (7)$$

The Lagrangian of a planar snake robot is equivalent to the robot's kinetic energy T, which is calculated as

$$T = \frac{1}{2}(m\dot{\boldsymbol{x}}^T\dot{\boldsymbol{x}} + m\dot{\boldsymbol{y}}^T\dot{\boldsymbol{y}} + J\dot{\boldsymbol{\theta}}^T\dot{\boldsymbol{\theta}}) = \frac{1}{2}\dot{\bar{\boldsymbol{q}}}^T\bar{H}\dot{\bar{\boldsymbol{q}}}, \quad (8)$$

where J is the moment of inertia of a link. Inertia matrix $\bar{H}$ is defined as

$$\begin{aligned} \bar{H} &:= mJ_{\bar{q}x}^T J_{\bar{q}x} + mJ_{\bar{q}y}^T J_{\bar{q}y} + \bar{J}, \quad (9) \\ \bar{J} &= \operatorname{diag}(0, 0, J, ..., J) \in \mathbb{R}^{(n+2)\times(n+2)}. \end{aligned}$$

To take the viscous friction into account, a Rayleigh dissipation function is used. Let the coefficients of viscosity between the environment and link i be c_x in the x^i direction, c_y in the y^i direction, and c_θ in the rotational direction, which are equal for each link. The point of action of the viscous friction is assumed to be the CM of each link. Letting the rotation matrix that relates the local frame of link i and the global frame be $^G R_i$, the dissipation function for link i is then

$$\mathcal{R}_i = \frac{1}{2}\dot{\boldsymbol{x}}_i^T \, ^G R_i \begin{bmatrix} c_x & 0 \\ 0 & c_y \end{bmatrix} (^G R_i)^T \dot{\boldsymbol{x}}_i + \frac{1}{2}c_\theta\dot{\theta}_i^2. \quad (10)$$

By summing for all links, the dissipation function for the entire robot can be derived as

$$\mathcal{R} = \frac{1}{2}\dot{\bar{\boldsymbol{q}}}^T(C_{\text{tr}} + C_{\text{rot}})\dot{\bar{\boldsymbol{q}}} = \frac{1}{2}\dot{\bar{\boldsymbol{q}}}^T\bar{C}\dot{\bar{\boldsymbol{q}}}, \quad (11)$$

where

$$C_{\mathrm{tr}} = J_{\bar{q}xy}^T \begin{bmatrix} c_x C_\theta^2 + c_y S_\theta^2 & (c_x - c_y) S_\theta C_\theta \\ (c_x - c_y) S_\theta C_\theta & c_x S_\theta^2 + c_y C_\theta^2 \end{bmatrix} J_{\bar{q}xy},$$
(12)

$$C_{\mathrm{rot}} = \mathrm{diag}(0,\ 0,\ c_\theta,\ \cdots,\ c_\theta),$$
(13)

$$J_{\bar{q}xy} = \begin{bmatrix} J_{\bar{q}x}^T & J_{\bar{q}y}^T \end{bmatrix}^T.$$
(14)

Lagrange's equations of motion are then written as

$$\frac{d}{dt}\left(\frac{\partial T}{\partial \dot{\bar{q}}}\right)^T - \left(\frac{\partial T}{\partial \bar{q}}\right)^T + \left(\frac{\partial \mathcal{R}}{\partial \dot{\bar{q}}}\right)^T = \bar{E}\boldsymbol{\tau},$$
(15)

where $\bar{E} \in \mathbb{R}^{n \times (n-1)}$ is a coefficient matrix and $\boldsymbol{\tau} \in \mathbb{R}^{n-1}$ is the torque applied to the joints. After some tedious calculations, whose details are given in the literature [16], we get

$$\bar{H}\ddot{\bar{q}} + \bar{W}\mathrm{diag}(\dot{\bar{q}})\dot{\bar{q}} + \bar{C}\dot{\bar{q}} = \bar{E}\boldsymbol{\tau},$$
(16)

$$\bar{W} = J_{\bar{q}x}^T M \mathcal{J}_x + J_{\bar{q}y}^T M \mathcal{J}_y,$$

$$\mathcal{J}_x = \begin{bmatrix} O_{n\times 2} & -K C_\theta \end{bmatrix},$$

$$\mathcal{J}_y = \begin{bmatrix} O_{n\times 2} & -K S_\theta \end{bmatrix},$$

where $\bar{W}\mathrm{diag}(\dot{\bar{q}})\dot{\bar{q}}$ is the term for Coriolis and centrifugal forces.

For the purpose of controller design, it is more convenient to express the system in terms of joint angles instead of link orientations. Let q be defined as $q = [x_h \ \ y_h \ \ \theta_1 \ \ \phi^T]^T$. The generalized coordinates $\bar{q}$ and q are related by the equation

$$\dot{\bar{q}} = J_{q\bar{q}}\dot{q},$$

$$J_{q\bar{q}} = \mathrm{block\,diag}(I_2, L),$$

$$L = \begin{bmatrix} 1 & 0 & \cdots & 0 \\ 1 & 1 & \cdots & 0 \\ \vdots & \vdots & \ddots & \vdots \\ 1 & 1 & \cdots & 1 \end{bmatrix} \in \mathbb{R}^{n \times n}.$$
(17)

Substituting (17) into (16) and multiplying $J_{q\bar{q}}^T$ to both sides of (16) from the left, we get

$$H\ddot{q} + W\mathrm{diag}(J_{q\bar{q}}\dot{q})J_{q\bar{q}}\dot{q} + C\dot{q} = E\boldsymbol{\tau},$$
(18)

where

$$
\begin{aligned}
H &= J_{q\bar{q}}^T \bar{H} J_{q\bar{q}} \\
&= J_{q\bar{q}}^T \begin{bmatrix} mn & 0 & -m\mathbf{1}^T K S_\theta \\ 0 & mn & m\mathbf{1}^T K C_\theta \\ -m S_\theta K^T \mathbf{1} & m C_\theta K^T \mathbf{1} & \bar{H}_{22} \end{bmatrix} J_{q\bar{q}} \\
&= \begin{bmatrix} mn & 0 & -m\mathbf{1}^T K S_\theta L \\ 0 & mn & m\mathbf{1}^T K C_\theta L \\ -m L^T S_\theta K^T \mathbf{1} & m L^T C_\theta K^T \mathbf{1} & L^T \bar{H}_{22} L \end{bmatrix},
\end{aligned}
$$
(19)

$$\bar{H}_{22} = m(S_\theta K^T K S_\theta + C_\theta K^T K C_\theta) + J I_n,$$

$W = J_{q\bar{q}}^T \bar{W}$, $\quad C = J_{q\bar{q}}^T \bar{C} J_{q\bar{q}}$, $\quad$ and $\quad E = J_{q\bar{q}}^T \bar{E} = [O_{(n-1)\times 3}^T \quad I_{n-1}]^T$. Note that the multiplication of $J_{q\bar{q}}^T$ from the left is required to make the inertia matrix H symmetric.

For the work presented in later sections, it is convenient to combine the nonlinear term and viscous friction term:

$$H(\boldsymbol{q})\ddot{\boldsymbol{q}} + \boldsymbol{h}(\boldsymbol{q}, \dot{\boldsymbol{q}}) = E\boldsymbol{\tau},$$
(20)

where $\boldsymbol{h} = W\mathrm{diag}(J_{q\bar{q}}\dot{q})J_{q\bar{q}}\dot{q} + C\dot{\boldsymbol{q}}$.

III. Dynamic Manipulability and Singular Posture of a Snake Robot

In this section, we define the concept of the dynamic manipulability of a snake robot that obeys equations of motion (20). The purpose of defining the manipulability in the present study is to define the singular posture for snake robots without a lateral constraint. From this point of view, some simplification is adopted for the manipulability in an ordinary sense. Moreover, as we are also interested in the case that there is a free joint, the extension to such a case is also discussed.

3.1. Case of No Free Joint

We first note that H is symmetric and positive definite. Symmetry and positive semi-definiteness are obvious from the definition. The positive definiteness of H is therefore equivalent to full rankness, which is also easily observed. In fact, H drops rank if and only if $\bar{H}$ drops rank because $J_{q\bar{q}}$ is of column full rank. If $\bar{H}$ drops rank, there must be a vector $\boldsymbol{v}$ that satisfies $\boldsymbol{v}^T \bar{H} \boldsymbol{v} = 0$. However, because all three matrices involved in the definition of H, namely $J_{\bar{q}x}^T J_{\bar{q}x}$, $J_{\bar{q}y}^T J_{\bar{q}y}$, and $\bar{J}$, are positive semi-definite, such $\boldsymbol{v}$ must satisfy $\boldsymbol{v}^T \bar{J} \boldsymbol{v} = 0$, which only holds when $\boldsymbol{v}$ is of the form $\boldsymbol{v} = [a \ \ b \ \ 0 \ \ \cdots \ \ 0]^T$, and for such $\boldsymbol{v}$, we have

$$
\begin{aligned}
\boldsymbol{v}^T \bar{H} \boldsymbol{v} &= m\boldsymbol{v}^T J_{\bar{q}x}^T J_{\bar{q}x} \boldsymbol{v} + m\boldsymbol{v}^T J_{\bar{q}y}^T J_{\bar{q}y} \boldsymbol{v} \\
&= (a^2 + b^2)mn > 0,
\end{aligned}
$$
(21)

which shows that $\bar{H}$ is of full rank and therefore positive definite.

The following proposition is useful for the following manipulations.

Proposition 1. *Considering the division of a positive definite matrix H,*

$$H = \begin{bmatrix} H_{11} & H_{12} \\ H_{21} & H_{22} \end{bmatrix}, \tag{22}$$

$$H_{11} \in \mathbb{R}^{3\times 3}, \ H_{12} \in \mathbb{R}^{3\times(n-1)},$$
$$H_{21} = H_{12}^T, \ H_{22} \in \mathbb{R}^{(n-1)\times(n-1)},$$

it follows that H_{11}, H_{22}, $H_{11} - H_{12}H_{22}^{-1}H_{21}$, *and* $H_{22} - H_{21}H_{11}^{-1}H_{12}$ *are symmetric and positive definite.*

Proof. Let the principal minor of order k of H be Δ_k. Because H is positive definite, $\Delta_k > 0$ for $k = 1, 2, ..., n+2$ is concluded from Sylvester's criterion. The positive definiteness of H_{11} follows from $\Delta_1 > 0$, $\Delta_2 > 0$, $\Delta_3 > 0$. As this implies that H_{11} is non-singular, the following transformation holds:

$$T \begin{bmatrix} H_{11} & H_{12} \\ H_{21} & H_{22} \end{bmatrix} T^T = \begin{bmatrix} H_{11} & O_{3\times(n-1)} \\ O_{(n-1)\times 3} & H_{22} - H_{21}H_{11}^{-1}H_{12} \end{bmatrix}, \tag{23}$$

$$T = \begin{bmatrix} I_3 & O_{3\times(n-1)} \\ -H_{21}H_{11}^{-1} & I_{n-1} \end{bmatrix}.$$

Because T is of full rank, the positive definiteness of THT^T is equivalent to that of H on the one hand. On the other hand, because THT^T is a block diagonal matrix, its positive definiteness is equivalent to the positive definiteness of the two diagonal block matrices. Therefore, $H_{22} - H_{21}H_{11}^{-1}H_{12}$ is positive definite.

For the positive definiteness of H_{22}, we consider the matrix

$$\begin{bmatrix} H_{22} & H_{21} \\ H_{12} & H_{11} \end{bmatrix}.$$

This is the inertia matrix for other general coordinates,

$$z = \begin{bmatrix} O_{(n-2)\times 3} & I_{n-2} \\ I_3 & O_{3\times(n-2)} \end{bmatrix} q,$$

and because this is a mere exchange of coordinates, it is obvious that this transformation from q to z does not change the positive definiteness of the inertia matrix. Therefore, according to arguments similar to those made for H_{11} and $H_{22} - H_{21}H_{11}^{-1}H_{12}$, the positive definiteness of H_{22} and $H_{11} - H_{12}H_{22}^{-1}H_{21}$ is proven. $\square$

Using division (22), the equation of motion (20) can be written as

$$H_{11}\ddot{w} + H_{12}\ddot{\phi} + h_1 = 0_3, \tag{24}$$

$$H_{12}\ddot{w} + H_{22}\ddot{\phi} + h_2 = \tau, \tag{25}$$

where h_1 and h_2 are the first three rows and next $n-1$ rows of h respectively. Because H_{22} is invertible, the second equation (25) can be solved for $\ddot{\phi}$ as

$$\ddot{\phi} = -H_{22}^{-1}(H_{21}\ddot{w} + h_2) + H_{22}^{-1}\tau. \tag{26}$$

By substituting this into (24), we have

$$(H_{11} - H_{12}H_{22}^{-1}H_{21})\ddot{w} - H_{12}H_{22}^{-1}(h_2 - \tau) + h_1 = 0_3. \tag{27}$$

Therefore, by setting τ as

$$\tau = h_2 - \bar{\tau} - H_{22}H_{12}^{\dagger}h_1, \tag{28}$$

where $H_{12}^{\dagger}$ is the pseudo-inverse of H_{12}, we have

$$(H_{11} - H_{12}H_{22}^{-1}H_{21})\ddot{w} = H_{12}H_{22}^{-1}\bar{\tau}, \tag{29}$$

if H_{12} is of full rank. We admit (29) for the time being. From this equation, it is concluded that if the norm of $\bar{\tau}$ is restricted to $\|\bar{\tau}\| \leq 1$, $\ddot{w}$ is in an ellipsoid, which is called the manipulability ellipsoid, in three-dimensional space. Using the manipulability ellipsoid, we define the singular posture of a snake robot as follows.

Definition 1. *A singular posture of a snake robot is a posture for which the manipulability ellipsoid is embedded in a two-dimensional subspace of three-dimensional space of possible* $\ddot{w}$.

Note that if $n \leq 3$, the ellipsoid is contained on a plane or a line and its volume becomes zero, which means that a certain direction of $\ddot{w}$ is not achievable regardless of the robot shape. We therefore only consider the case of $n \geq 4$ in what follows.

The manipulability ellipsoid illustrates the available head acceleration $\ddot{w}$ using the joint torques that satisfy $\|\tau\| = 1$. If (and only if) it is not possible to produce the head acceleration in some direction, then the ellipsoid does not have any 'thickness' in that direction. In such cases, the ellipsoid is a two-dimensional ellipse or a one-dimensional line segment, if there is one more such infeasible direction. Therefore, if the robot is in a singular posture, it means that there is at least one direction in which we cannot accelerate the head.

The singular values of $(H_{11} - H_{12}H_{22}^{-1}H_{21})^{-1}H_{12}H_{22}^{-1}$ characterize the ellipsoid and a larger singular value implies better manipulability. Let the singular values of the matrix be σ_1, σ_2, σ_3. The manipulability criterion D is defined as

$$D = \min\{\sigma_1, \sigma_2, \sigma_3\}. \tag{30}$$

In the present work, however, we are especially interested in the singular posture of a snake robot,

which means the minimum of the singular value is zero. This is equivalent to the case that $(H_{11} - H_{12}H_{22}^{-1}H_{21})^{-1}H_{12}H_{22}^{-1}$ drops rank. Because H_{22} and the Schur complement $H_{11} - H_{12}H_{22}^{-1}H_{21}$ are non-singular from Proposition 1, singularity implies that H_{12} drops rank. For this reason, we consider the singular values of H_{12} instead of those of $(H_{11} - H_{12}H_{22}^{-1}H_{21})^{-1}H_{12}H_{22}^{-1}$ as the manipulability criterion. Let the singular values of H_{12} be $\lambda_1,\ \lambda_2,\ \lambda_3$. The manipulability criterion R is defined as

$$R = \min\{\lambda_1, \lambda_2, \lambda_3\}. \tag{31}$$

It is obvious that the following theorem holds.

Theorem 1. *If $n \geq 4$, the singular posture of a snake robot is the posture with $D = R = 0$.*

This can also be considered as another definition of the singular posture.

We mentioned that (29) holds if H_{12} is of full rank and (29) does not hold in general if H_{12} drops rank. This is because $H_{12}H_{12}^{\dagger} = I$ does not hold in this case and $\boldsymbol{\tau}$ defined in (28) does not necessarily cancel the effect of $\boldsymbol{h}_1$. We therefore think of the singular posture as the posture that makes (29) invalid for some $\boldsymbol{h}_1$.

In contrast to the definition given by Date et al. [10], which explicitly considers the lateral constraint force and tries to give a larger value when the lateral constraint force is weaker, our definition does not consider the lateral constraint in any way. This is better suited to real robots with an inevitable side slip, giving a larger manipulability value to the shape that can produce a stronger propulsion force. Additionally, the settings of Date et al. [10] do not consider motion in the θ_h direction. This is because, in the settings of Date et al., θ_h cannot be controlled arbitrarily. Using our criteria, we can explicitly take motion in the θ_h direction into consideration. Note that it is also easy not to consider this motion. Changing how the matrix H is divided into block matrices, to $H_{11} \in \mathbb{R}^{2\times2}, H_{12} \in \mathbb{R}^{2\times n}$, and $H_{22} \in \mathbb{R}^{n\times n}$, suffices to achieve this.

Note also that our manipulability criteria do not depend on the model of the friction force. Although the property of the friction affects the locomotion performance of snake robots, it does not change the direction in which the robot can accelerate its head.

3.2. Case of a Free Joint

As can be expected from the previous discussion, only a few modifications and cautions are required to

consider the case that a joint is free. Letting the joint k be free, the equation of motion becomes

$$H(\boldsymbol{q})\ddot{\boldsymbol{q}} + \boldsymbol{h}(\boldsymbol{q}, \dot{\boldsymbol{q}}) = \tilde{E}'\tilde{\boldsymbol{\tau}}, \tag{32}$$

where we delete the kth element of $\boldsymbol{\tau}$ and kth column of E to make $\bar{\boldsymbol{\tau}}$ and $\tilde{E}'$, respectively.

The division of the equations of motion (24) and (25) is motivated by the fact that there is no external force for the first three elements, but not for other elements. In this case, however, the $k + 3$th element also does not have any external force term. It is therefore necessary to gather those elements without external forces into the first four elements. Let the selection matrix S be defined as

$$S = \begin{bmatrix} I_3 & O_{3\times(n-1)} \\ O_{(n-1)\times3} & S_{\text{sub}} \end{bmatrix},$$
$$S_{\text{sub}} = \begin{bmatrix} \boldsymbol{e}_k & \boldsymbol{e}_1 & \boldsymbol{e}_2 & \cdots & \boldsymbol{e}_{k-1} & \boldsymbol{e}_{k+1} & \cdots & \boldsymbol{e}_{n-1} \end{bmatrix}, \tag{33}$$

where $\boldsymbol{e}_i$ is an $n - 1$ dimensional unit vector whose ith element is 1. It is easily seen that S is orthogonal; i.e., $S^T = S^{-1}$. A new general coordinate $\tilde{\boldsymbol{q}}$ is defined as

$$\tilde{\boldsymbol{q}} = S\boldsymbol{q}. \tag{34}$$

By this transformation of coordinates, the equation of motion becomes

$$\tilde{H}\ddot{\tilde{\boldsymbol{q}}} + \tilde{\boldsymbol{h}} = \tilde{E}\tilde{\boldsymbol{\tau}}, \tag{35}$$

where

$$\tilde{H} = SHS^T, \ \tilde{\boldsymbol{h}} = S\boldsymbol{h}, \ \tilde{E} = S\bar{E}. \tag{36}$$

Note that $\bar{H}$ is also symmetric and positive definite. The transformed equation of motion can then be divided as

$$\tilde{H}_{11}\ddot{\tilde{\boldsymbol{w}}} + \tilde{H}_{12}\ddot{\tilde{\boldsymbol{\phi}}} + \tilde{\boldsymbol{h}}_1 = \boldsymbol{0}_4, \tag{37}$$

$$\tilde{H}_{12}\ddot{\tilde{\boldsymbol{w}}} + \tilde{H}_{22}\ddot{\tilde{\boldsymbol{\phi}}} + \tilde{\boldsymbol{h}}_2 = \tilde{\boldsymbol{\tau}}, \tag{38}$$

where

$$\tilde{\boldsymbol{w}} = \begin{bmatrix} x_h & y_h & \theta_h & \phi_k \end{bmatrix}^T, \tag{39}$$

$$\tilde{\boldsymbol{\phi}} = \begin{bmatrix} \phi_1 & \cdots & \phi_{k-1} & \phi_{k+1} & \cdots & \phi_{n-1} \end{bmatrix}^T. \tag{40}$$

The sub-block matrices of $\tilde{H}$ are defined as

$$\tilde{H} = \begin{bmatrix} \tilde{H}_{11} & \tilde{H}_{12} \\ \tilde{H}_{21} & \tilde{H}_{22} \end{bmatrix}, \tag{41}$$
$$\tilde{H}_{11} \in \mathbb{R}^{4\times4}, \ \tilde{H}_{12} \in \mathbb{R}^{4\times(n-2)},$$
$$\tilde{H}_{21} = \tilde{H}_{12}^T, \ \tilde{H}_{22} \in \mathbb{R}^{(n-2)\times(n-2)},$$

and $\tilde{\boldsymbol{h}}_1$ and $\tilde{\boldsymbol{h}}_2$ are the first four elements and remaining $n-2$ elements of $\tilde{\boldsymbol{h}}$, respectively.

The key to the definition of the manipulability criterion R in the previous subsection is Proposition 1. In the case that a joint is free, it is obvious from the definition of $\tilde{H}$ (36) and the proof of Proposition 1 that the following is true.

Proposition 2. *Consider the division of $\tilde{H}$ in (41). Then $\tilde{H}_{11}$, $\tilde{H}_{22}$, $\tilde{H}_{11} - \tilde{H}_{12}\tilde{H}_{22}^{-1}\tilde{H}_{21}$, and $\tilde{H}_{22} - \tilde{H}_{21}\tilde{H}_{11}^{-1}\tilde{H}_{12}$ are symmetric and positive definite.*

Because of this proposition, the same discussion can be had and we define the manipulability criteria $\tilde{D}$ and $\tilde{R}$ as

$$\tilde{D} = \min\{\tilde{\sigma}_1, \tilde{\sigma}_2, \tilde{\sigma}_3, \tilde{\sigma}_4\}, \quad \tilde{R} = \min\{\tilde{\lambda}_1, \tilde{\lambda}_2, \tilde{\lambda}_3, \tilde{\lambda}_4\}, \tag{42}$$

where $\tilde{\sigma}_i$, $(i = 1, 2, 3, 4)$ are four singular values of $(\tilde{H}_{11} - \tilde{H}_{12}\tilde{H}_{22}^{-1}\tilde{H}_{21})^{-1}\tilde{H}_{12}\tilde{H}_{22}^{-1}$ and $\tilde{\lambda}_i$, $(i = 1, 2, 3, 4)$ are those of $\tilde{H}_{12}$. Note that we only consider the case of $n \geq 5$. If $n \leq 4$, the manipulability ellipsoid is embedded in a three-dimensional hyperplane of the four-dimensional space of possible $\ddot{\tilde{\boldsymbol{w}}}$. Therefore, $n \geq 5$ is required for $\ddot{\tilde{\boldsymbol{w}}}$ to be assigned freely. In the case that $n \geq 5$, the singular posture is defined as follows.

Definition 2. *A singular posture of a snake robot with a free joint is the posture with $\tilde{D} = \tilde{R} = 0$, if the number of links n satisfies $n \geq 5$.*

IV. Manipulability Analysis

In this section, we analyze the manipulability of a snake robot for special cases. Intuitively, manipulability defines some kind of 'controllability' of the robot, though it is not the same as the concept of actual controllability.

In the following analysis, we assume that $\theta_1 = 0$ rad without loss of generality.

4.1. Case that All Joint Angles are Zero

If all joint angles are zero, the shape of the snake robot is a straight line. It is obvious that H_{12} drops rank in this case. To see this, we recall the detail of H in (19). Because $\boldsymbol{\theta} = \boldsymbol{0}_n$, it holds that $S_\theta = O_{n \times n}$ and therefore $-m\boldsymbol{1}^T K S_\theta L = \boldsymbol{0}_n^T$, which implies that the first row of H_{12} is $\boldsymbol{0}_{n-1}^T$.

The same is true in the case that joint k is free because the first row of $\tilde{H}_{12}$ is generated by eliminating the kth element of the first row of H_{12}.

Table 1. Parameters of the robot

m	0.182 kg	$2l$	0.12 m
J	0.22 kgm^2	n	10

(a) Manipulability criterion D

(b) Manipulability criterion R
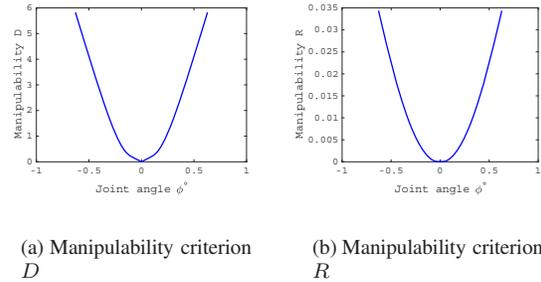
Fig. 2. Manipulability criteria D and R.

4.2. Case that All Joint Angles are the Same

In more general cases, it is difficult to handle the general form of H_{12}. In this subsection, we examine the manipulability for numerical examples. The settings of the robot are given in Table 1.

Joint angles are set to share the same angle ϕ^o. The two manipulability criteria D and R are plotted in Fig. 2 against $\phi^o \in [-\pi/5, \pi/5]$. Note that if $|\phi^o| = \pi/5$ rad, then the robot forms a closed loop, which is a regular decagon.

The figure shows that although the manipulability criteria D and R take small values if all joints share the same angle, they are zero only at $\phi^o = 0$ rad. However, we note that this does not contradict the previous result in [20], that the shape of an arc does not satisfy a sufficient condition for accessibility. We first note the difference in control points. In the present paper, we consider the control of the head and the orientation of the first link, instead of the CM and mean orientation. It is possible that the head is controllable and at the same time the CM is not. Moreover, the result in [20] only states a sufficient condition and not any necessary condition, while our result can be recognized as a necessary condition.

As an example with a free joint, the fifth joint is set to be free. The manipulability criteria become as shown in Fig. 3. Note the difference in the exponent of the labels of the vertical axes between Figs. 2 and 3. As can be expected, with a free joint, manipulability becomes much lower because there are fewer inputs. However, the criteria share the same qualitative features; i.e. they are zero only if $\phi^o = 0$ rad.

(a) Manipulability criterion D

(b) Manipulability criterion R
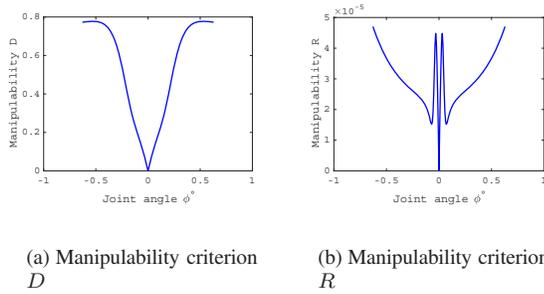
Fig. 3. Manipulability criteria D and R in the case that joint 5 is free.

(a) Manipulability criterion D

(b) Manipulability criterion R

Fig. 4. Manipulability criteria D and R. The snake robot's shape is a serpenoid curve with $T_s = 1.5$.

4.3. Serpenoid Curves

The serpenoid curve, which was proposed by Hirose [1], is the *de facto* standard for the shape of a snake robot. Serpenoid curves are curves whose curvature is determined by the sine function. This family of curves is expected to be useful in avoiding singular postures. To approximate the serpenoid curve for a snake robot, joint angles are determined using the three parameters α, v, and T_s:

$$\phi_i = \frac{2\pi T_s}{n} \alpha \sin\left(vt - \frac{2\pi T_s}{n} i \right), \quad i = 1, \cdots, n-1.$$
(43)

Among the parameters, v is the time frequency. The spatial frequency $2\pi T_s/n$ is defined for a snake robot to form exactly T_s periods of the curve. The maximum angle between the curve and the direction of movement will be α, which we call the winding angle.

In Fig. 8, the manipulability criteria with $T_s = 1.5$ are shown for various α while in Fig. 9 those with $\alpha = \pi/4$ are shown for various T_s. The shape of the snake is shown for $T_s = 1.5$ and $\alpha = \pi/16$, $\pi/8$, $\pi/4$, $\pi/2$ in Fig. 6, and for $\alpha = \pi/4$ and $T_s = 0.5$, 1.0, 1.5, 2.0 in Fig. 7. It is confirmed that by employing serpenoid curves, we can prevent the robot from having a singular shape, except in the trivial cases of $\alpha = 0$ and $T_s = 0$. Note that because H does not depend on any velocity components, the manipulability criteria do not depend on v.

Figures 8 and 9 show the results for the case that the fifth joint is free. As in Section 4.2, the overall values are much smaller than those in the case without a free joint because of the loss of input. However, they become zero only at $\alpha = 0$ or $T_s = 0$.
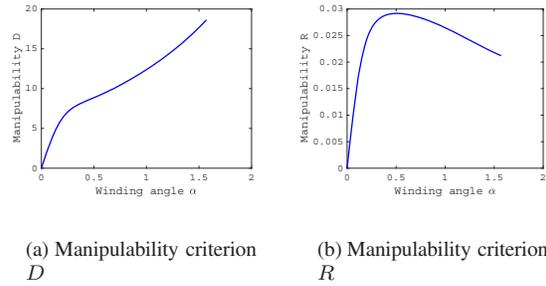

(a) Manipulability criterion D

(b) Manipulability criterion R

Fig. 5. Manipulability criteria D and R. The snake robot's shape is a serpenoid curve with $\alpha = \pi/4$.

(a) $\alpha = \pi/16 \simeq 0.20$ rad

(b) $\alpha = \pi/8 \simeq 0.39$ rad

(c) $\alpha = \pi/4 \simeq 0.79$ rad

(d) $\alpha = \pi/2 \simeq 1.57$ rad
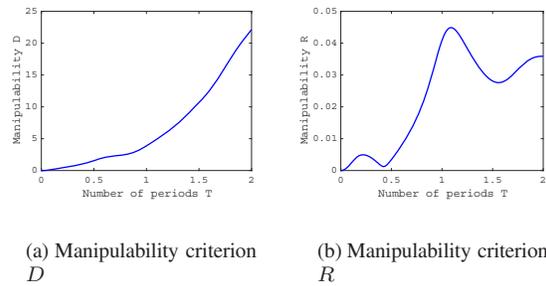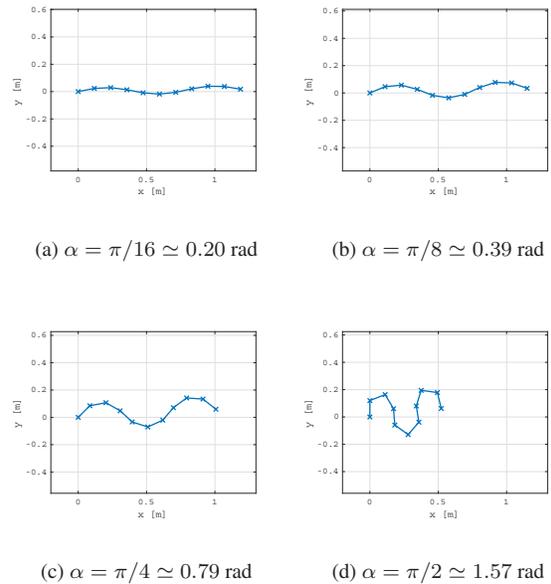
Fig. 6. Snake robot with a serpenoid shape for $T_s = 1.5$.

(a) $T_s = 0.5$ (b) $T_s = 1.0$

(c) $T_s = 1.5$ (d) $T_s = 2.0$

Fig. 7. Snake robot with a serpenoid shape for $\alpha = \pi/4$.
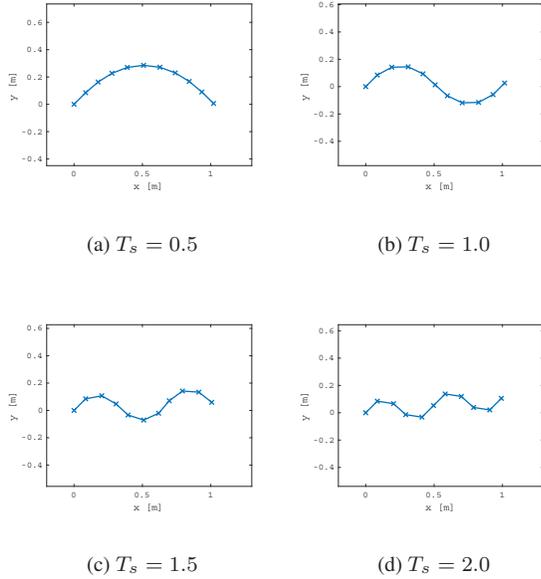
(a) Manipulability criterion D

(b) Manipulability criterion R
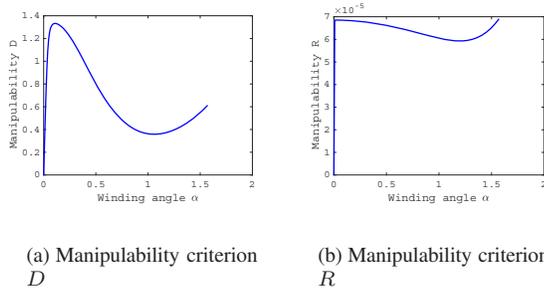
Fig. 8. Manipulability criteria D and R. The snake robot's shape is a serpenoid curve with $T_s = 1.5$. The fifth joint is free.


(a) Manipulability criterion D

(b) Manipulability criterion R
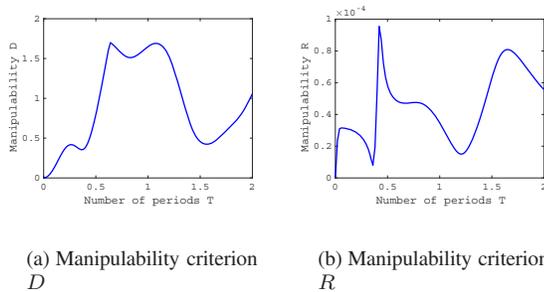
Fig. 9. Manipulability criteria D and R. The snake robot's shape is a serpenoid curve with $\alpha = \pi/4$. The fifth joint is free.

V. Uncontrollability with Isotropic Friction: Integrability Point of View

It is well known that a snake needs anisotropy in friction to move without any objects to push around [23]. This was also theoretically shown [20] in that with isotropic friction, the CM of the snake robot is uncontrollable. However, because of the difference in control points, it is not clear whether the same holds true in our case. In fact, the dynamic manipulability is not zero unless all joint angles are zero, regardless of the friction, as shown in the previous section. Note that the dynamic manipulability is based on a local property of the head acceleration that is defined by the inertial properties and cannot consider friction.

Before going into detail, we recall that the first three rows of the equation of motion (24) have no external forces. It can therefore be thought that there is a set of acceleration level constraints (i.e., second-order constraints). These constraints are referred to as non-holonomic if they cannot be completely integrated, and the constraints being non-holonomic is a necessary condition for the system to be controllable. If the constraints are holonomic (i.e., if they can be integrated), there are conservation laws, which make it impossible to have the states be arbitrary.

In this section, we give the condition for these constraints to be integrable and show that two of these second-order constraints can be integrated once to gain first-order constraints. The property of the second-order constraint that it can be integrated once is called partial integrability [24]. Partial integrability does not formally prove that the robot cannot move to a desired point and, for this proof, it is required to show that the first-order constraints are also holonomic. However, the existence of the integral for the second-order constraints shows that at least it satisfies a necessary condition for the robot to be uncontrollable.

The following discussion can also be applied to the case that one of the joints is free, with the same modifications made in Section 3.2. Because the introduction of a free joint only makes the calculation a little more tedious and does not change the conclusion, we omit the discussion.

5.1. Partial Integrability Condition

Let the general coordinate be divided as $\boldsymbol{q} = [\boldsymbol{q}_1^T \quad \boldsymbol{q}_2^T]^T$, where $\boldsymbol{q}_1 \in \mathbb{R}^k$ and $\boldsymbol{q}_2 \in \mathbb{R}^{n+2-k}$, $k \in \{1, 2, 3\}$. If $k = 3$, then $\boldsymbol{q}_1 = \boldsymbol{w}$ and $\boldsymbol{q}_2 = \boldsymbol{\phi}$. For this division, the equation of motion can be restated as

$$H_1 \boldsymbol{q} + \boldsymbol{W}_1 + C_1 \dot{\boldsymbol{q}} = \boldsymbol{0}_k, \tag{44}$$

$$H_2 \boldsymbol{q} + \boldsymbol{W}_2 + C_2 \dot{\boldsymbol{q}} = E_2 \boldsymbol{\tau}, \tag{45}$$

where H_1 and H_2 are the matrices of the first k and remaining $n + 2 - k$ rows of H, respectively. C_1, C_2, W_1, W_2, and E_2 are defined in the same way from C, $W = W \operatorname{diag}(J_{q\bar{q}}\dot{q})J_{q\bar{q}}\dot{q}$, and E. Note that the first k rows of E are a zero matrix. From the derivation of Lagrange's equation of motion, it holds that

$$W_1 = \dot{H}_1 \dot{q} - \frac{1}{2} \left\{ \frac{\partial}{\partial q_1}(\dot{q}^T H \dot{q}) \right\}^T. \qquad (46)$$

Being free from external forces, (44) represents the second-order constraints. For the integrability of the constraints, the following theorem holds.

Theorem 2. *The necessary and sufficient conditions for (44) to be partially integrable without any integrating factor are as follows.*

1. *$\frac{\partial}{\partial q_1}(\dot{q}^T H \dot{q}) = 0$; i.e., elements of q_1 are cyclic.*
2. *There exists a function $g_2(q)$ that satisfies $C_1(q) = \frac{\partial g_2}{\partial q}$.*

Proof. We first show the necessity. If (44) is integrable, there exists a function $g : \mathbb{R}^{n+2} \times \mathbb{R}^{n+2} \times \mathbb{R} \to \mathbb{R}^k$ such that

$$\dot{g}(q, \dot{q}, t) = \frac{\partial g}{\partial q}\dot{q} + \frac{\partial g}{\partial \dot{q}}\ddot{q} + \frac{\partial g}{\partial t} = \text{(l.h.s. of (44))}. \qquad (47)$$

From (44), it is clear that $\dot{g}$ does not contain t explicitly. It should therefore hold that $\partial g / \partial t = \text{const.}$; i.e., it holds that

$$g(q, \dot{q}, t) = g_1(q, \dot{q}) + k_1 t, \qquad (48)$$

where k_1 is a k-dimensional constant vector.

We consider the case that $\dot{q} = 0_n$. In this case, because $W(q, \dot{q}) + C(q)\dot{q} = 0_n$, we have

$$H_1 \ddot{q} = 0_k, \qquad (49)$$

on the one hand, and on the other hand,

$$\dot{g}(q, 0_n, t) = \frac{\partial g_1}{\partial \dot{q}}\ddot{q} + k_1. \qquad (50)$$

By comparison, it is deduced that

$$k_1 = 0_k, \quad \frac{\partial g_1}{\partial \dot{q}} = H_1. \qquad (51)$$

We therefore have

$$g(q, \dot{q}, t) = g_2(q) + H_1 \dot{q}. \qquad (52)$$

By taking the time derivative, we get

$$\dot{g}(q, \dot{q}, t) = H_1 \ddot{q} + \dot{H}_1 \dot{q} + \frac{\partial g_2}{\partial q}\dot{q}. \qquad (53)$$

From (46) to (44), we have

$$H_1 \ddot{q} + \dot{H}_1 \dot{q} - \frac{1}{2} \left\{ \frac{\partial}{\partial q_1}(\dot{q}^T H \dot{q}) \right\}^T + C_1 \dot{q} = 0_k. \qquad (54)$$

A comparison of the above two equations gives

$$\frac{\partial g_2}{\partial q}\dot{q} = C_1 \dot{q} - \frac{1}{2} \left\{ \frac{\partial}{\partial q_1}(\dot{q}^T H \dot{q}) \right\}^T$$
$$\Leftrightarrow \frac{1}{2} \left\{ \frac{\partial}{\partial q_1}(\dot{q}^T H \dot{q}) \right\}^T + \left\{ \frac{\partial g_2}{\partial q} - C_1 \right\} \dot{q} = 0_k. \qquad (55)$$

Noting that the first term on the left-hand side is the second-order term of $\dot{q}$ and that the second term is the first-order term, it holds that

$$\frac{\partial}{\partial q_1}(\dot{q}^T H \dot{q}) = 0_k, \quad \frac{\partial g_2}{\partial q} = C_1(q). \qquad (56)$$

This completes the proof of necessity.

The proof of sufficiency is almost trivial because if the conditions are satisfied, (44) becomes

$$H_1 \ddot{q} + \dot{H}_1 \dot{q} + \frac{\partial g_2}{\partial q}\dot{q} = 0_k \qquad (57)$$

$$\frac{d}{dt}\{H_1 \dot{q} + g_2\} = 0_k. \qquad (58)$$

The partial integral of (44) is $g = H_1 \dot{q} + g_2$. $\square$

Note that similar results for a manipulator with passive joints have been reported [24] but they were obtained without considering the friction between the robot and environment. With the friction, the condition to be partially integrable becomes more complicated as seen in Theorem 2.

5.2. Complete Integrability Condition

If the second-order constraint is partially integrable, it holds that

$$H_1(q)\dot{q} + g_2(q) + k = 0, \qquad (59)$$

for some constant vector k, which is determined from the initial conditions. If this first-order differential equation is also integrable, we say that the constraint

is completely integrable [24]. The integrability of this equation is equivalent to the integrability of

$$H_1(\boldsymbol{q})\dot{\boldsymbol{q}} + \boldsymbol{g}_2(\boldsymbol{q}) = \boldsymbol{0} \iff H_1(\boldsymbol{q})d\boldsymbol{q} + \boldsymbol{g}_2(\boldsymbol{q})dt = \boldsymbol{0},$$
(60)

where $d\boldsymbol{q} = [dq_1, \ ..., \ dq_{n+2}]^T$. The necessary and sufficient condition of this differential equation to be integrable is given by the Frobenius theorem [25] as follows.

Theorem 3. *Let Δ be the distribution that spans the kernel space of $\begin{bmatrix} H_1 & \boldsymbol{g} \end{bmatrix}$; i.e., $\Delta(\boldsymbol{q}) = \ker \begin{bmatrix} H_1(\boldsymbol{q}) & \boldsymbol{g}(\boldsymbol{q}) \end{bmatrix}$ for any $\boldsymbol{q}$. The necessary and sufficient condition for (60) to be integrable is that the distribution Δ is involutive.*

5.3. Integrability Test for Second-order Constraints

From (19), it is clear that $\boldsymbol{q}_1 = [x_h \ \ y_h]^T$ satisfies the first condition of Theorem 2 because H does not depend on x_h or y_h.

For further investigation, we need to write down the elements of C_1. Although the whole C is too complex to write down, the first two rows (i.e., C_1) are a little less complex and can be expressed as

$$C_1 = \begin{bmatrix} c_{11} & c_{12} & \boldsymbol{c}_{13}^T \\ c_{21} & c_{22} & \boldsymbol{c}_{23}^T \end{bmatrix},$$
(61)

$$c_{11} = c_x \| \cos \boldsymbol{\theta} \|^2 + c_y \| \sin \boldsymbol{\theta} \|^2,$$

$$c_{12} = c_{21} = (c_x - c_y) \sin \boldsymbol{\theta}^T \cos \boldsymbol{\theta},$$

$$c_{23} = c_x \| \sin \boldsymbol{\theta} \|^2 + c_y \| \cos \boldsymbol{\theta} \|^2,$$

$$\boldsymbol{c}_{13}^T = \{ -c_x \cos \boldsymbol{\theta}^T C_\theta K S_\theta - c_y \sin \boldsymbol{\theta}^T S_\theta K S_\theta,$$
$$+ (c_x - c_y) \sin \boldsymbol{\theta}^T C_\theta K C_\theta \} L,$$

$$\boldsymbol{c}_{23}^T = \{ -(c_x - c_y) \cos \boldsymbol{\theta}^T S_\theta K S_\theta,$$
$$+ c_y \sin \boldsymbol{\theta}^T S_\theta K C_\theta + c_y \cos \boldsymbol{\theta}^T C_\theta K C_\theta \} L.$$

It is still difficult to check the second condition of Theorem 2 in general, but some simplification can be made if $c_x = c_y$.

In the case of $c_x = c_y = c$, we have

$$c_{11} = nc, \ c_{12} = c_{21} = 0, \ c_{22} = nc,$$
(62)

$$\boldsymbol{c}_{13}^T = -c \boldsymbol{1}^T K S_\theta L,$$
(63)

$$\boldsymbol{c}_{23}^T = c \boldsymbol{1}^T K C_\theta L.$$
(64)

The ith elements of $\boldsymbol{c}_{13}$ and $\boldsymbol{c}_{23}$ are calculated as

$$(\boldsymbol{c}_{13})_i = -cl \sum_{j=i}^{n} (2n - 2j + 1) \sin \theta_j$$
$$= -cl \sum_{j=i}^{n} (2n - 2j + 1) \sin \left(\theta_1 + \sum_{q=1}^{j-1} \phi_q \right),$$
(65)

$$(\boldsymbol{c}_{23})_i = cl \sum_{j=i}^{n} (2n - 2j + 1) \cos \theta_j$$
$$= cl \sum_{j=i}^{n} (2n - 2j + 1) \cos \left(\theta_1 + \sum_{q=1}^{j-1} \phi_q \right).$$
(66)

These results show that a function $\boldsymbol{g}_2$ that is defined by

$$\boldsymbol{g}_2 = \begin{bmatrix} g_{21} \\ g_{22} \end{bmatrix},$$

$$g_{21} = ncx_h + cl \sum_{j=1}^{n} (2n - 2j + 1) \cos \left(\theta_1 + \sum_{q=1}^{j-1} \phi_q \right),$$

$$g_{22} = ncy_h + cl \sum_{j=i}^{n} (2n - 2j + 1) \sin \left(\theta_1 + \sum_{q=1}^{j-1} \phi_q \right)$$
(67)

satisfies the second condition of Theorem 2.

It is concluded that, in the case of $c_x = c_y$, because the first two rows of the equation of motion (44) with $k = 2$ are partially integrable, there exists a conservation law $\boldsymbol{g}(\boldsymbol{q}) = H_1 \dot{\boldsymbol{q}} + \boldsymbol{g}_2 = \text{const}$. This suggests that the robot is uncontrollable under isotropic friction also in the case that the control point is the head, instead of at the CM. The formal proof of the uncontrollability requires examination of whether the first-order constraints $\boldsymbol{g}(\boldsymbol{q}) = \text{const.}$ satisfy the condition of Theorem 3. However, because of the complexity of the system, the examination is difficult even for some special cases with small n.

VI. Simulation Study

6.1. Comparison between Two Criteria

A simulation is performed

1. to show that of the two proposed manipulability criteria, R is better for determining whether the posture is close to singular,
2. to show that the postures with all joints having the same angle are not generally singular postures,

3. and to check the conservation of g that was shown in the previous section for the case of isotropic friction.

We use the controller based on partial feedback linearization designed for tracking the head trajectory. Note that, in the present paper, we only consider the case without any free joint. Also note that because we use the isotropic friction setting in this simulation, it is expected that the control will fail at some point.

6.1.1. Partial Feedback Linearization

Let $\mathcal{H}$ be the Schur complement of the block H_{22} in (22):

$$\mathcal{H} = H_{11} - H_{12}H_{22}^{-1}H_{21}. \qquad (68)$$

Because $\mathcal{H}$ is invertible from Proposition 1, (27) can be solved for $\ddot{\boldsymbol{w}}$ as

$$\ddot{\boldsymbol{w}} = -\mathcal{H}^{-1}\boldsymbol{h}_1 + \mathcal{H}^{-1}H_{12}H_{22}^{-1}\boldsymbol{h}_2 - \mathcal{H}^{-1}H_{12}H_{22}^{-1}\boldsymbol{\tau}. \qquad (69)$$

From (69), if we define $\boldsymbol{\tau}$ as

$$\boldsymbol{\tau} = H_{22}H_{12}^{\dagger}\mathcal{H}\{\ddot{\boldsymbol{w}}^r + K_v(\dot{\boldsymbol{w}}^r - \dot{\boldsymbol{w}}) + K_p(\boldsymbol{w}^r - \boldsymbol{w})\}$$
$$- H_{22}H_{12}^{\dagger}(\boldsymbol{h}_1 - H_{12}H_{22}^{-1}\boldsymbol{h}_2)$$
$$+ H_{22}(I - H_{12}^{\dagger}H_{12})\boldsymbol{\kappa}, \qquad (70)$$

where K_v and K_p are 3×3 positive-definite matrices and $\boldsymbol{\kappa}$ is an arbitrary $n-1$-dimensional vector, we have

$$\ddot{\boldsymbol{w}} = \ddot{\boldsymbol{w}}^r + K_v(\dot{\boldsymbol{w}}^r - \dot{\boldsymbol{w}}) + K_p(\boldsymbol{w}^r - \boldsymbol{w}), \qquad (71)$$

or in other words

$$(\ddot{\boldsymbol{w}}^r - \ddot{\boldsymbol{w}}) + K_v(\dot{\boldsymbol{w}}^r - \dot{\boldsymbol{w}}) + K_p(\boldsymbol{w}^r - \boldsymbol{w}) = \boldsymbol{0}, \qquad (72)$$

whenever H_{12} is of row full rank. This equation implies the asymptotic convergence of $\boldsymbol{w}^r - \boldsymbol{w}$ to $\boldsymbol{0}$. Note that, although the snake robot is an underactuated system, there is some redundancy in controlling $\boldsymbol{w}$, which might be modulated through the vector $\boldsymbol{\kappa}$.

6.1.2. Use of Redundancy

Although (71) implies asymptotic convergence of $\boldsymbol{w}$ to $\boldsymbol{w}^r$, the internal stability of the system is questionable. For single-input-single-output systems, zero dynamics will play an important role in the analysis of stability, but for multiple-input-multiple-output systems with redundancy, the theory of zero dynamics is under development [26], and it seems that

we currently lack important tools with which to ensure our system's stability.

Nonetheless, one important insight is given by Theorem 3 of [20]: the controller must be time variant for our system to be stable. The following lemma holds as a direct consequence.

Lemma 1. *The vector $\boldsymbol{\kappa}$ in (70) must be time variant to render the system stable.*

Although there seems only a small theoretical guidepost for the design of $\boldsymbol{\kappa}$, it is natural to use periodical functions because we usually need a 'gait' that continues ad infinitum. Following common practice in the field of snake robots, we use the serpenoid curve in the determination of $\boldsymbol{\kappa}$. As shown in Section 4.3, with the serpenoid curve, it is expected to be possible to avoid the singularity.

By substituting (70) and (71) into (25), we can eliminate $\ddot{\boldsymbol{w}}$ and $\boldsymbol{\tau}$. Multiplication by H_{22}^{-1} from the left leads to

$$\ddot{\boldsymbol{\phi}} + H_{12}^{\dagger}\boldsymbol{h}_1 + (I - H_{12}^{\dagger}H_{12})(H_{22}^{-1}\boldsymbol{h}_2 - \boldsymbol{\kappa})$$
$$+ P\{\ddot{\boldsymbol{w}}^r + K_v(\dot{\boldsymbol{w}}^r - \dot{\boldsymbol{w}}) + K_p(\boldsymbol{w}^r - \boldsymbol{w})\} = \boldsymbol{0}, \qquad (73)$$

where $P = (H_{22}^{-1}H_{12} - H_{12}^{\dagger}\mathcal{H})$. Let us assume that the convergence of $\boldsymbol{w}$ to $\boldsymbol{w}^r$ is already achieved; i.e., $\dot{\boldsymbol{w}}^r - \dot{\boldsymbol{w}} = \boldsymbol{0}$ and $\boldsymbol{w}^r - \boldsymbol{w} = \boldsymbol{0}$. The system then becomes

$$\ddot{\boldsymbol{\phi}} + H_{12}^{\dagger}\boldsymbol{h}_1 + (I - H_{12}^{\dagger}H_{12})(H_{22}^{-1}\boldsymbol{h}_2 - \boldsymbol{\kappa}) = \boldsymbol{0}. \qquad (74)$$

Let $\boldsymbol{\kappa}$ be defined as

$$\boldsymbol{\kappa} = H_{22}^{-1}\boldsymbol{h}_2 - \boldsymbol{u}, \qquad (75)$$

where $\boldsymbol{u}$ is an arbitrary vector. We then have

$$\ddot{\boldsymbol{\phi}} + H_{12}^{\dagger}\boldsymbol{h}_1 + (I - H_{12}^{\dagger}H_{12})\boldsymbol{u} = \boldsymbol{0}. \qquad (76)$$

By multiplying by $(I - H_{12}^{\dagger}H_{12})$ from the left and noting that $(I - H_{12}^{\dagger}H_{12})$ is idempotent (i.e., $(I - H_{12}^{\dagger}H_{12})^2 = (I - H_{12}^{\dagger}H_{12})$) and $(I - H_{12}^{\dagger}H_{12})H_{12}^{\dagger} = O$ from the definition of the pseudo-inverse, we have

$$(I - H_{12}^{\dagger}H_{12})(\ddot{\boldsymbol{\phi}} + \boldsymbol{u}) = 0. \qquad (77)$$

Note that the $(n-1)$-by-$(n-1)$ matrix $(I - H_{12}^{\dagger}H_{12})$ can never be of full rank. In fact, because $H_{12}^{\dagger}H_{12}$ is idempotent, its eigenvalues are restricted to values of 1 (multiplicity $\mathrm{rank}H_{12}$) and 0 (multiplicity $n - 1 - \mathrm{rank}H_{12}$). Furthermore, because $H_{12}^{\dagger}H_{12}$ is symmetric, it can be diagonalized by a unitary transformation and the same transformation does not alter the identity

matrix. As a consequence, it is confirmed that the eigenvalues of $(I - H_{12}^\dagger H_{12})$ are 1 (multiplicity $n - 1 - \mathrm{rank}H_{12}$) and 0 (multiplicity $\mathrm{rank}H_{12}$). Because $\mathrm{rank}H_{12} \leq 3$, we have $\mathrm{rank}(I - H_{12}^\dagger H_{12}) \leq n - 4$. Therefore, (77) does not ensure that $\ddot{\phi} + u = 0$. However, it is expected that the input (75) tries to achieve $\ddot{\phi} + u = 0$ as closely as possible, using the redundancy that remains after achieving trajectory tracking.

As a consequence, we set κ as

$$\begin{aligned} \kappa &= H_{22}^{-1}h_2 - u \\ u &= -\ddot{\phi}^r - R_v(\dot{\phi}^r - \dot{\phi}) - R_p(\phi^r - \phi), \end{aligned} \tag{78}$$

where R_v and R_p are $(n-1) \times (n-1)$ positive-semidefinite matrices. The reference for the joint angles ϕ^r is determined according to (43).

6.1.3. Result of Control Based on Partial Feedback Linearization

The simulation uses the same parameters used in Section IV and listed in Table 1; i.e., the number of links is $n = 10$, the length of each link is $2l = 0.12$ m, and the mass of each link is $m = 0.182$ kg. The friction coefficients are set to $c_x = c_y = 0.5$ Ns/m and $c_\theta = 7.2 \times 10^{-5}$ Nms. The matrices used in the controller (70) and (78) are defined as

$$\begin{aligned} K_v &= 6.0I_3, \quad K_p = 6.2I_3, \\ R_v &= 0.041I_{n-1}, \quad R_p = 0.079I_{n-1}. \end{aligned} \tag{79}$$

The reference w^r is

$$w^r = \begin{bmatrix} 0.1t & 0 & 0 \end{bmatrix}^T. \tag{80}$$

The parameters for the serpenoid curve are

$$\alpha = \frac{\pi}{3}, \ T_s = 1, \ v = 0.18. \tag{81}$$

Tuning these parameters requires much care. First, because w should converge to w^r quickly, K_v and K_p should be relatively large; i.e., larger than R_v and R_p. However, if they are too large, the state will diverge within several computational steps. The serpenoid parameters are chosen such that the speed of the CM is close to the reference speed of the head. These settings are empirically the best for our robot and the reference trajectory.

The initial state η_0 is set as

$$\eta_0 = \begin{bmatrix} w_0 \\ \phi_0 \\ 0_{n+2} \end{bmatrix}, \ w_0 = \begin{bmatrix} 0 \\ 0 \\ 0 \end{bmatrix}, \ \phi_0 = \frac{\pi}{6}1_{n-1}. \tag{82}$$

(a) Manipulability criteria D and R (b) Manipulability criterion R and torque norm $\|\tau\|$
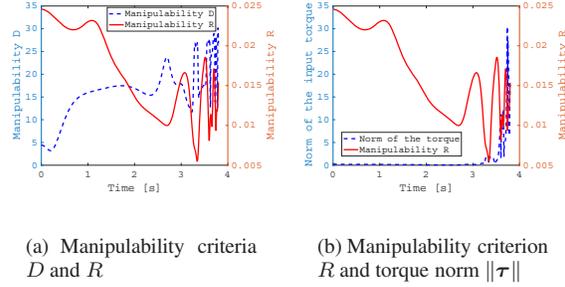
Fig. 10. Manipulability criteria and norm of the torque input.

Note that, according to previous wisdom based on the study of snake robots with lateral constraints, the snake robot is uncontrollable in the initial state.

The two manipulability criteria D and R are shown in Fig. 10(a). The norm of the torque input $\|\tau\|$ is shown in Fig. 10(b) along with the manipulability criterion R. It is seen that although D takes a very small value at first, $\|\tau\|$ and R do not. However, before $\|\tau\|$ becomes very large, only R has a small value at around $t = 3.44$ s. The postures of the robot at $t = 0.0$ s and $t = 3.44$ s are shown in Fig. 11. Although it is not clear from the visual appearance that the robot is close to adopting a singular posture, the conclusion that the robot is close to having a singular posture is consistent with the fact that $\|\tau\|$ becomes large after $t = 3.44$ s.

Figure 12 presents the value of each element of $g = H_1\dot{q} + g_2$ along with the manipulability criterion R. According to the discussion in Section 5.3, g must be conserved during the simulation. It is obvious that both elements of g are conserved in the first couple of seconds.

However, both elements of g decrease sharply after $t = 3.44$ s, at which time R reaches its lowest value. This implies that R correctly characterizes the singular posture and if R is too small it becomes difficult to simulate the robot's motion accurately. These results also support our conclusion that R is better suited as a metric indicating how close the snake robot is to its singular posture.

Figure 11 also shows that within 3.44 seconds of movement, the snake head follows the indicated reference trajectory. It is therefore concluded that the posture for which all joints share the same joint angle is not generally a singular posture and is controllable at least locally.

(a) Initial robot posture

(b) Robot posture at the time of lowest R
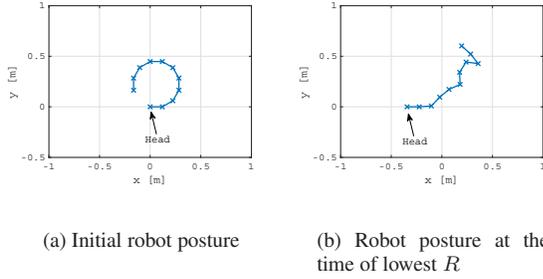
Fig. 11. Robot postures at $t = 0$ s and $t = 3.44$ s.

(a) First conservative

(b) Second conservative
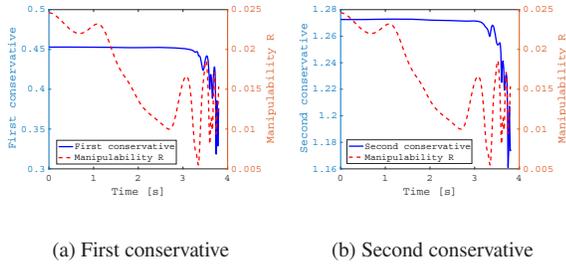
Fig. 12. Two conservatives defined in Section 5.3 for the case of isotropic friction.

6.2. Manipulability Analysis of Head Trajectory Tracking Control

In this subsection, the state-of-the-art head trajectory tracking controller proposed by the authors [27] is tested using our proposed manipulability criteria. The control method is based on a Lyapunov-like function:

$$V(\boldsymbol{w}, \dot{\boldsymbol{w}}, \dot{\boldsymbol{\phi}}) = \|(\dot{\boldsymbol{w}}^r - \dot{\boldsymbol{w}}) + K_{w1}(\boldsymbol{w}^r - \boldsymbol{w})\|^2_{K_{w2}} \\ + \|\dot{\boldsymbol{\phi}}^r - \dot{\boldsymbol{\phi}}\|^2_{K_\phi}, \quad (83)$$

where $\|\boldsymbol{x}\|_K = \boldsymbol{x}^T K \boldsymbol{x}$ for any vector $\boldsymbol{x}$ and a positive-definite matrix K. The control input $\boldsymbol{\tau}$ is defined to reduce the value of V. Although we use the serpenoid curve for $\boldsymbol{\phi}^r$, the produced body shape can be far from it. This is especially true if the singular values of K_ϕ are set to be smaller than those of K_{w1} and K_{w2}, which is often the case because achieving $\boldsymbol{w} \to \boldsymbol{w}^r$ is the first priority.

Although the main task of achieving $\boldsymbol{w} \to \boldsymbol{w}^r$ cannot be realized exactly, the advantage of this control method is that it is robust against the existence of a passive joint as shown in [27]. With only a little modification, the method can be used for a snake robot with a passive joint and the same level of tracking
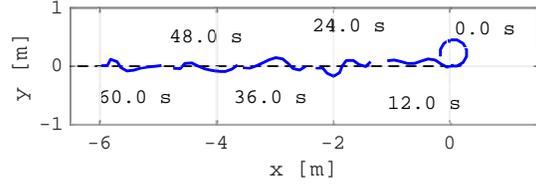

Fig. 13. Motion of the snake robot with head trajectory tracking control [27]. The dashed line is the reference path of the head.

(a) Manipulability D
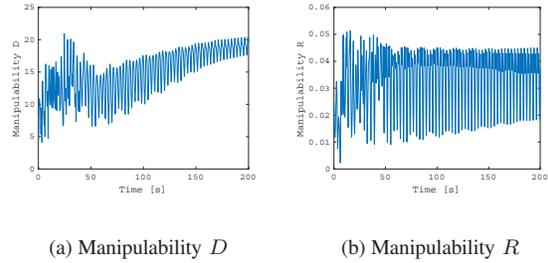
(b) Manipulability R

Fig. 14. Manipulability criteria for straight trajectory tracking.

performance can be attained. In what follows, we analyze the manipulability of the robot with and without a passive joint.

The parameters of the snake robot were set to those in the previous subsection 6.1.3. The reference $\boldsymbol{w}^r$ is also the same and the gain matrices are set as

$$K_{w1} = \mathrm{diag}(2, 2, 3), \; K_{w2} = \mathrm{diag}(400, 400, 45), \\ K_\phi = \mathrm{diag}(10, 20, ..., 20). \quad (84)$$

The $(1, 1)$ element of K_ϕ was set to be smaller than the others to facilitate using the first joint to adjust the head angle. The serpenoid parameters for $\boldsymbol{\phi}^r$ were $\alpha = \pi/6$, $v = 2$, and $T = 1.5$. The initial state was set to be the same as in Section 6.1.3, i.e., the shape of the snake robot was a circle at first.

6.2.1. Without Any Passive Joint

The motion of the robot without any passive joint for the first 60 s is shown in Fig. 13. The dashed line is the reference path and it can be seen that the control law [27] succeeded in head tracking with small error relative to the length of the snake robot, without converging to a singular posture. The manipulability criteria are shown in Fig. 14. This also confirms the success of the avoidance of singular postures.
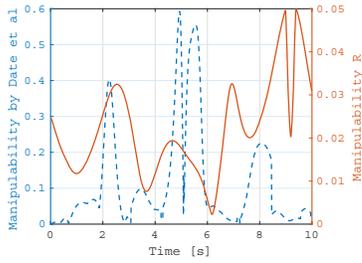
Fig. 15. Comparison of the criterion proposed by Date et al. and our criterion R, which has been shown to be better than the manipulability criterion D in detecting a singularity. The dashed line refers to the manipulability criterion of Date et al. while the solid line refers to R.

6.2.2. Comparison with an Existing Criterion [10]

To clarify that our manipulability criterion R, which was shown to be better for describing a singularity, has properties different from those of the criterion proposed by Date et al. [10], we make a comparison using the data obtained in Section 6.2.1. Note that, although the manipulability criterion proposed by Date et al. is used to evaluate properties other than R, it can also be used to detect a singularity of a snake robot with wheel constraints. The robot is assessed to be in a singular posture if the manipulability reaches zero.

In Fig. 15, the manipulability criterion proposed by Date et al. [10] and R are plotted for the time interval $t \in [0, 10]$. It is seen that at the initial posture, R becomes positive but the manipulability criterion of Date et al. reaches zero. Because the trajectory tracking task was successfully performed with this initial posture, it is clear that the manipulability criterion of Date et al. is not appropriate to detect the singularity for our settings.

6.2.3. With a Passive Joint

Let us assume that the fifth joint is passive. The motion of the robot for the first 60 s is shown in Fig. 16. The fifth joint is shown by a cross mark while the dashed line is the reference path. Again, it is seen that the control law [27] allows head tracking with small error relative to the length of the snake robot, without converging to a singular posture. The manipulability criteria are shown in Fig. 17. The figure confirms the avoidance of singular postures even if one of the joints is passive.
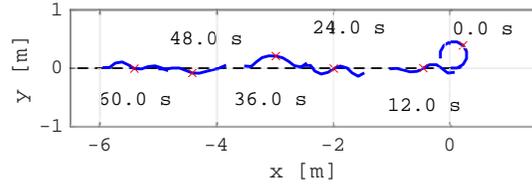

Fig. 16. Motion of a snake robot with head trajectory tracking control [27]. The fifth joint, which is shown by a cross mark, is set to be passive. The dashed line is the reference path of the head.


(a) Manipulability D (b) Manipulability R
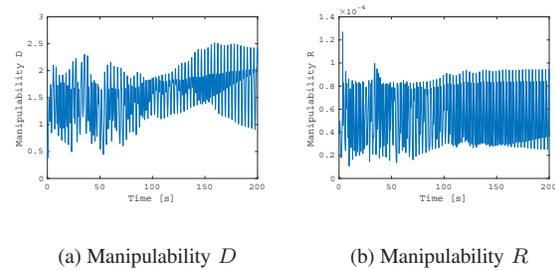
Fig. 17. Manipulability criteria for straight trajectory tracking in the case that the fifth joint is passive.

6.3. Analysis of Head Trajectory Tracking on a Physics Engine

To show the validity of our manipulability definition in a more realistic environment, the motion of a snake robot in a physics engine is analyzed. As the environment, we used Vortex running on V-REP. The robot model on V-REP is shown in Fig. 18.

The robot was composed of $n = 8$ links with equal length of $2l = 0.176$ m, equal mass of 0.417 kg, and equal moment of inertia of 1.20×10^{-3} kgm^2. The anisotropy in friction was achieved by placing a pair of passive wheels on each link. The Coulomb friction model was employed between the wheel and the floor, instead of the viscous friction that is used in the controller model. To estimate the general velocity $\dot{q}$, the pseudo-differential that is defined by the transfer function $2\pi f_c s / (2\pi f_c \ s + 1)$ was used. The cut-off frequency f_c was set to 10 Hz. All the parameters on the controller, including the reference trajectory and initial joint angles, are the same as those in Section 6.2.

Figure 19 shows the trajectory of the head. The solid line is for x_h and the dashed line is for y_h. The dotted lines show the references x_h^r and y_h^r. The manipulability criteria are shown in Fig. 20 and images capturing the movement of the snake robot during the first 60 s are shown in Fig. 21. It is seen that the robot successfully avoids the singular posture. Our criteria
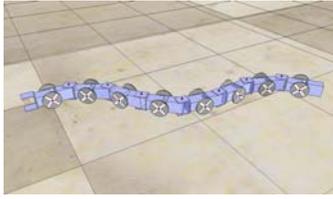
Fig. 18. Model of the snake robot in V-REP.
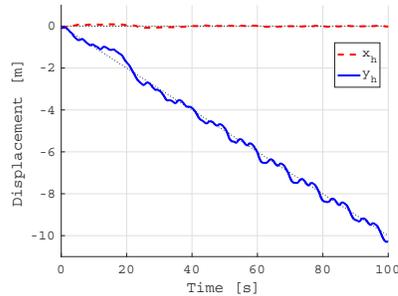
Fig. 19. Trajectory of the head position. The solid line and dashed line show x_h and y_h, respectively. The dotted lines refer to the references.
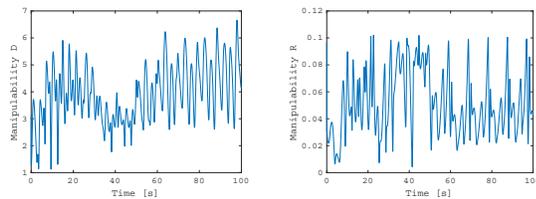
(a) Manipulability D (b) Manipulability R

Fig. 20. Manipulability criteria for the simulation using the physical engine.

show this success clearly, despite the difference in the model that it assumes, including the difference in the friction model.

VII. Conclusion

We defined the dynamic manipulability of a snake robot without a lateral constraint with the aim of future application to tracking the head trajectory. The singular posture of the snake robot was examined using the dynamic manipulability. Of the two manipulability criteria D and R, R was shown to be more suitable for detecting a singularity, though both become zero if and only if the robot is in a singular posture. Because we are interested in constructing a head tracking

control strategy that can also be used in the case of a malfunctioning joint, these criteria were also examined in the case that one of the joints is free. The quantitative properties of the manipulability criteria are different if there is a free joint, as is expected because there are fewer usable inputs. However, we observed the same qualitative property as in the case without free joints; i.e., the criteria are zero only if the robot has a straight line shape among the shapes that we tested. The manipulability criteria express only local properties that are determined only by inertial properties. The criteria therefore cannot be used to clarify the effect of friction; however, they can be used regardless of the type of friction. Furthermore, uncontrollability of the robot in the case of isotropic friction is, though only partially, explained from the point of view of integrability.

From the results of our simulation, we conjecture that the partial feedback linearization technique is not suitable for the head trajectory tracking control of a snake robot without a lateral constraint because it is too sensitive to parameter settings. We are now working at designing a suitable control strategy for the head trajectory tracking control of snake robots without a lateral constraint. Moreover, we are interested in making the control robust against joint failure and, as a typical case, we will consider the case that a joint becomes free owing to a problem in future work. Furthermore, we are interested in completing our proof on the uncontrollability of the head trajectory under isotropic friction.

REFERENCES

1. Hirose, S., *Biologically Inspired Robots: Snake-Like Locomotors and Manipulators*. Oxford University Press (1993).
2. Takemori, T., M. Tanaka, and F. Matsuno, "Gait Design for a Snake Robot by Connecting Curve Segments and Experimental Demonstration," *IEEE Trans. Robot.* Vol. 34, No. 5, 2018.
3. Rollinson, D. and H. Choset, "Pipe Network Locomotion with A Snake Robot," *J. Field Robotics*, Vol. 33, No. 3, pp. 322-336 (2016).
4. Baba, T., Y. Kameyama, T. Kamegawa, and A. Gofuku, "A snake robot propelling inside of a pipe with helical rolling motion," *SICE Annu. Conf.*, Taipei, Taiwan, pp. 2319-2325 (2010)
5. Prautsch, P., T. Mita, and T. Iwasaki, "Analysis and control of a gait of snake robot," *Trans. Electr. Electron. J.*, Vol. 120-D, pp. 372-381 (2000).
6. Date, H., Y. Hoshi, M. Sampei, and S. Nakaura, "Locomotion Control of a Snake Robot with Constraint Force Attenuation," *Proc. Amer. Control Conf.*, Arlington, VA, pp. 113-118 (2001).
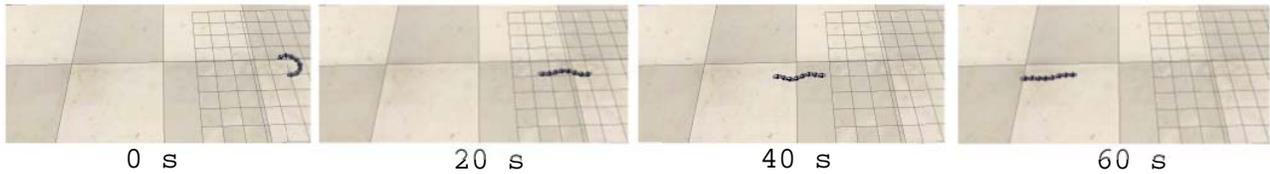
Fig. 21. Captured images of the simulation in V-REP.

7. Matsuno, F. and K. Mogi, "Redundancy controllable system and control of snake robots based on kinematic model," *Proc. IEEE Confe. Decis. Control*, Sydney, Australia, pp. 4791-4796 (2000).

8. Matsuno, F. and H. Sato "Trajectory tracking control of snake robots based on dynamic model," *Proc. IEEE Int. Conf. Robot. Autom.*, Barcelona, Spain, pp. 3040-3045 (2005).

9. Tanaka, M. and K. Tanaka, "Singularity Analysis of a Snake Robot and an Articulated Mobile Robot with Unconstrained Links," *IEEE Trans. Control Syst. Technol.*, Vol.24, No.6, pp. 2070-2081 (2016).

10. Date, H., Y. Hoshi and M. Sampei, "Locomotion Control of a Snake-like Robot based on Dynamic Manipulability," *Proc. IEEE/RSJ Int. Conf. Intell. Robot. Syst.*, Takamatsu, Japan, Vol. 3, pp. 2236-2241 (2000).

11. Tanaka, M. and K. Tanaka, "Control of a Snake Robot for Ascending and Descending Steps," *IEEE Trans. Robot.*, Vol.31, No.2 (2015).

12. Tsukano, H., M. Tanaka, and F. Matsuno, "Control of a Snake Robot on a Cylindrical Surface Based on a Kinematic Model," *IFAC Proc.*, Vol.42, No.16, pp. 699-704 (2009).

13. Korayem, M.H., A.M. Shafei, and H.R. Shafei, "Dynamic modeling of nonholonomic wheeled mobile manipulators with elastic joints using recursive Gibbs-Appell formulation," *Scientia Iranica B*, Vol.19, No.4, pp. 1092-1104 (2012).

14. Hrdina, J., A. NáVrat, P. Vašík, and R. Matoušek, "CGA-based robotic snake control," *Advances Appl. Clifford Algebras*, Vol.27, No.1, pp.621-632 (2017).

15. Saito, M., M. Fukaya, and T. Iwasaki, "Serpentine Locomotion with Robotic Snakes," *IEEE Control Syst. Mag.*, Vol. 22, No. 1, pp. 64-81 (2002).

16. Ariizumi, R. and F. Matsuno, "Dynamic Analysis of Three Snake Robot Gaits," *IEEE Trans. Robot.*, Vol. 33, No. 5, pp. 1075-1087 (2017).

17. Liljebäck, P., I.U. Haugstuen, and K.Y. Pettersen, "Path Following Control of Planar Snake Robots Using a Cascaded Approach," *IEEE Trans. Control Syst. Technol.*, Vol. 20, No. 1, pp. 111–126 (2012).

18. Liljebäck, P., K.Y. Pettersen, Ø. Stavdahl, and J.T. Gravdahl, "Lateral undulation of snake robots: a simplified model and fundamental properties," *Robotica*, Vol. 31, No. 7, pp. 1005-1036 (2013).

19. Hicks, G. and K. Ito, "A Method for Determination of Optimal Gaits With Application to a Snake-Like Serial-Link Structure," *IEEE Trans. Autom. Control,*, Vol. 50, No. 9, pp. 1291-1306 (2005).

20. Liljebäck, P., K. Pettersen, Ø. Stavdahl, and J. Gravdahl, "Controllability and Stability Analysis of Planar Snake Robot Locomotion," *IEEE Trans. Autom. Control*, Vol. 56, No. 6, pp. 1365-1380 (2011).

21. Tanaka, M. and F. Matsuno, "Control of snake robots with switching constraints: trajectory tracking with moving obstacle," *Adv. Robot.*, Vol.28, No. 6 (2014).

22. Ariizumi, R., M. Tanaka, and F. Matsuno, "Analysis and heading control of continuum planar snake robot based on kinematics and a general solution thereof," *Adv. Robot.*, Vol. 30, No. 5, pp. 301-314 (2016).

23. Gray, J., "The Mechanism of Locomotion in Snakes," *J. Exp. Biol.*, Vol. 23, No. 2, pp. 101-123 (1946).

24. Oriolo, G. and Y. Nakamura, "Control of Mechanical Systems with Second-Order Nonholonomic Constraints: Underactuated Manipulators," *Proc. IEEE Confe. Decis. Control*, Brighton, UK, pp. 2398-2403 (1991).

25. Isidori, A., *Nonlinear Control Systems*, Springer (1995).

26. Isidori, A., "The zero dynamics of a nonlinear system: From the origin to the latest progresses of a long successful story," *Eur. J. Control*, Vol. 19, pp. 369-378 (2013).

27. Ariizumi, R., R. Takahashi, M. Tanaka, and T. Asai, "Head-Trajectory-Tracking Control of a Snake Robot and Its Robustness Under Actuator Failure," *IEEE Trans. Control Syst. Technol.*, doi: 10.1109/TCST.2018.2866964.